Electrochemical Materials and Technologies

ARTICLE

Electrochemical Materials and Technologies

eISSN: 2949-0561

Cite this: Electrochem. Mater. Technol. 2 (2023) 20232009

Received: 18 November 2022
Accepted: 5 December 2022
Published online: 28 December 2022

DOI: 10.15826/elmattech.2023.2.009

Influence of caprolactam on the tin electrodeposition on a dispersed carbon support and preparation of Pt/(SnO_2/C) catalysts

Dmitry Mauer [a *], Sergey Belenov [ab]

Composite SnO_2/C materials obtained by electrodeposition of tin on Vulcan XC72 particles were used to fabricate a platinum catalyst for the oxygen electroreduction reaction (ORR). Thermogravimetry and X-ray diffraction methods made it possible to determine the composition of materials and the size of platinum and tin oxide crystallites. The use of the SnO_2/C composite obtained in the presence of ε-caprolactam (CPL) as a support made it possible to increase the electrochemically active surface area (ESA) of platinum and the mass activity of the Pt/SnO_2/C catalyst in ORR.

keywords: electrocatalysis, tin oxide, oxygen reduction reaction, caprolactam

1. Introduction

At present, platinum-containing electrocatalysts are of great interest in connection with their application in low-temperature fuel cells (PEMFCs) [1]. The operation of PEMFC is based on electrochemical reactions of oxidation of a reducing agent (for example, H_2) and reduction of an oxidizing agent (O_2) that occur on the highly dispersed catalyst surface.

The characteristics of such catalysts depend primarily on their composition and structure. The most efficient are electrocatalysts consisting of platinum nanoparticles (NPs) deposited on the carbon supports surface [2–4]. Recently, interest has grown in the preparation and study of nanostructured oxide-carbon materials that could replace pure carbon as a stable support for platinum NPs. It was suggested development of the method we proposed earlier [5, 6] of the electrolytic formation of platinum nanoparticles on dispersed carbon support as applied to the electrodeposition of other metals, which are significantly inferior thermodynamic stability to platinum. Formation of nanostructured oxide-carbon materials that are of great interest as support for platinum NPs. The fact is that metal oxide/carbon composite materials can have several advantages over pure carbon precisely as a support. One of the most important aspects is the strengthening of the bond between the platinum nanoparticles and the support, a more uniform spatial distribution of the nanoparticles, and, as a result, an increase in the ESA, activity, and stability of the catalyst. Of particular interest, in our opinion, may be nanostructured composite SnO_x/C supports, which are promising for use in various fields of electrochemical energy, including electrocatalysis [7–8].

In recent years, tin oxide has often been presented as a promising support for platinum nanoparticles [9]. In the articles Pt/SnO_2/C demonstrate high characteristics in the reactions of oxidation of alcohols [10–11] and in the reaction of oxygen reduction [12–14]. To obtain composite supports for platinum catalysts, it is necessary to use depositing methods an oxide component on carbon,

a: Chemistry Department, Southern Federal University, Rostov-on-Don 344090, Russia
b: Prometheus R&D LLC, Rostov-on-Don 344091, Russia

* Corresponding author: dima333000@yandex.ru

which would subsequently provide the possibility of supplying/withdrawing electrons to/from supported platinum NPs. It was noted in [7] that the tin obtained by pulsed dispersion of the tin electrode spontaneously oxidizes to SnO_x, improving the catalytic properties of the obtained Pt/(SnO_2/C) material. The SnO_2/C system has good electronic conductivity. The study of the electrochemical behavior of Pt/SnO_2/C catalysts in compared to the Pt/C analog indicated a decrease in the electrooxidation potential of methanol and ethanol with a simultaneous increase in the process rate [7].

It is known that the nanosized structure of SnO_2 crystals, which determines the high specific surface area of the oxide, affects the performance of various devices (gas sensors, photo sensors, photocatalysts, antistatic coatings, sensitized dyes, and solar cells) created using this material [15]. Various types of SnO_2 particles and films can be prepared using pyrolysis [16, 17], laser ablation [18, 19], the sol–gel synthesis [20], and homogeneous deposition methods [21, 22].

Nanoscale control of morphology as applied to SnO_2 based materials on remains a complex problem that could be solved using electrochemical methods for its production. We believe that the SnO_2/C composite obtained by electrolytic tin deposition followed by spontaneous oxidation of metal nanoparticles can be a promising support for platinum, provided that the oxide is formed in the form of nanosized particles strongly fixed on the dispersed carbon surface. A well-known method of influencing the microstructure of the sediment is the use of organic compounds that can significantly modify the surface of the growing sediment.

One of the promising additives that affect the deposited metal surface structure is ε-caprolactam. Previously, it was shown that it not only changes the electrodeposition kinetics of metals such as copper [23] and nickel [24], but also improves the microstructure of the surface layer, determining the properties of the resulting coatings. Based on the above, the aim of this study was to investigate the effect of the addition of ε-caprolactam on the process of tin electrodeposition on carbon in suspension and on the morphological characteristics of the obtained SnO_2/C materials. Obtain platinum-containing catalysts based on synthesized SnO_2/C supports and study their microstructural and functional characteristics.

2. Experimental

For the preparation of PtSnO_2/C catalyst, the method of formaldehyde synthesis was used [25]. To determine the tin and platinum content in the materials, we used the thermal analysis method. The material was heat-treated for 30 minutes at 800 °C and then kept for 40 minutes in a desiccator to establish a constant mass, after which the mass of metals was determined.

Cyclic voltammetry (CV) was used to determine the electrochemical active surface area (ESA) of platinum as was described in the previous literature [26]. The electrochemical activity of the catalysts was studied by liner sweep voltammetry (LSV) [26]. The powder x-ray diffraction method on a laboratory source, an ARL X'TRA diffractometer with Bragg-Brentano geometry was used to determine the samples composition and the nanoparticles (crystallites) size of SnO_2 and Pt. Typical settings: 40 kV, 35 mA, 0.02-degree scan step in 2 theta. Recording speed from 4–8 degrees per minute. Phase analysis was performed based on data obtained from open sources, including using the Crystallography Open Database (COD) [27, 28]. The average crystallite diameter was determined using the Scherrer equation [29], into which the corresponding value of the FWHM peak was substituted:

$$D_{hkl} = \mathrm{K} \cdot \lambda / [\mathrm{FWHM} \cdot \cos(\Theta)] \quad (1)$$

where λ is the wavelength of monochromatic radiation; FWHM = peak full width at half maximum (in radians); D_{hkl} is the average thickness of the "stack" of reflecting planes in the region of coherent scattering, i.e., average crystallite diameter; ϑ is half of the angle of reflection; $K = 0.89$ is Scherrer's constant. To consider instrumental broadening, the diffractometer was preliminarily calibrated using a standard sample, which was a plate of polycrystalline annealed α-quartz with a grain size of 2 to 4 microns.

The peculiar morphological properties of the samples were studied by scanning electron microscopy (SEM) on a FE-SEM Zeiss SUPRA 25 instrument. To calculate the average particle size distribution were estimated sizes of 400 particles.

3. Results

Dispersed SnO_2/C systems were obtained by electrodeposition of tin on a dispersed carbon support from sulfate solutions by the method described in [17]. Electrodeposition modes (current value and process time) were chosen so that the amount of electricity passing through the system was the same and amounted to 33.6 C (Table 1). The reduced thermodynamic stability of nanosized metal particles caused the conversion of Sn/C to SnO_2/C due to interaction with dissolved oxygen during synthesis and air oxygen during filtering and drying of materials. The SnO_2/C compositions of the

Table 1 – Dependence of the mass fraction of tin in SnO_2/C on the concentration of tin sulfate and synthesis conditions.

$SnSO_4$ – grams per liter	Sample	*I*, A	τ, min	ω(Sn), %
0.25	SC-1	1.6	21	25.5 ± 3.5
	SC-2	6	5.6	35.0 ± 3.5
	SC-3	9	3.7	12.9 ± 1.5
0.25 + CPL*	SC_{CPL}-1	1.6	21	37.0 ± 3.5
	SC_{CPL}-2	6	5.6	26.5 ± 2.5
	SC_{CPL}-3	9	3.7	30.0 ± 3.0

*caprolactam

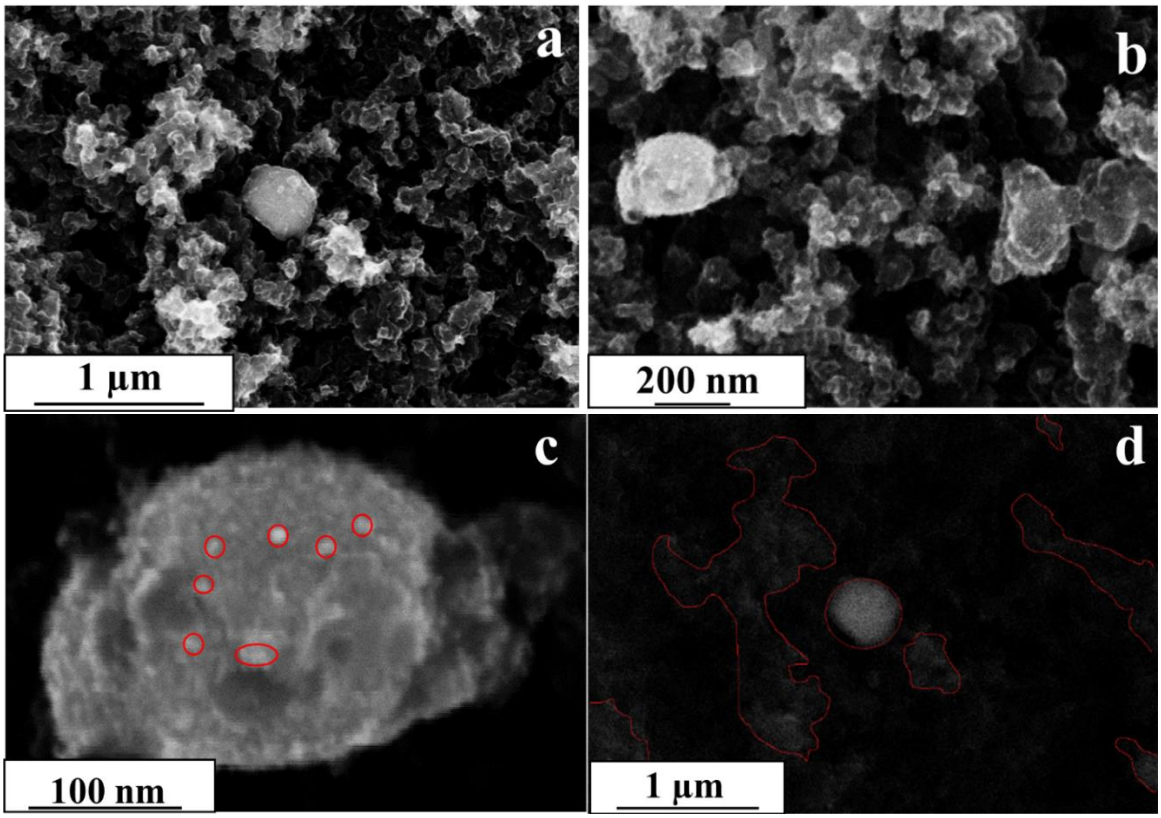

Figure 1 Photographs of the SC_{CPL}-2 samples surface (ω(Sn) = 26.5 %), obtained by scanning electron microscopy in the shooting reflected (a, b) and secondary electrons (c, d) mode.

materials obtained under different electrolysis conditions are shown in Table 1. Variation of the current regime showed that an increase in the salt concentration does not lead to a corresponding increase content of SnO_2 in the obtained material.

The ambiguity of the obtained results is explained by the difficult conditions of the synthesis, which are accompanied by gas evolution and heating of the solution, especially at high current values. SEM images of materials obtained in the reflected high-energy mode (Figure 1 a,b) and secondary low-energy electrons (Figure 1 c,d) show that the formation of both small tin oxide particles and large tin particles with a rough surface, which is typical for electrolytic tin deposits. Photographs in the Z-contrast mode (Figure 1 c,d), make it possible to distinguish particles by the mass of constituent elements. On this photograph lighter inclusions contain tin compounds (isolated fragments). When zooming in on the surface of tin large particles (Figure 1 c), smaller formations with size about 7 nm can be distinguished (Figure 1 c).

For samples obtained in the presence of caprolactam, a change in viscosity was observed; during filtration, it was necessary to resort to the centrifugation technique. These effects may be associated with the formation of a surfactant shell around carbon particles, which prevents them from sticking together. This can affect the particle

Table 2 – Composition of the studied samples of Pt/(SnO_2/C) catalysts.

Sample	ω(Sn), %	ω(Pt), %		Average crystallite size (XRD) Pt, nm	
		Estimated	Actual	SnO_2	Pt
PSC-1	25.5	20	17	3.0	3.8
PSC_{CPL}-2	26.5	20	19	2.2	2.2

size of deposited SnO_2 and Sn. The X-ray diffraction patterns of these materials contain peaks that can be attributed to the SnO_2 and Sn phases. The addition of caprolactam leads to a decrease in the size of tin crystallites from 3.0 nm to 2.2 nm (Table 2, Figure 2). In turn, the reflections in the XRD corresponding to the metallic tin phase are much narrower, and the estimate of the average crystallite size in this case cannot be carried out with sufficient accuracy.

The data obtained by X-ray diffraction are in good agreement with the SEM results, since the photographs contain well-defined light aggregates that can be attributed to large Sn particles with a size of more than a few hundred nanometers. The next stage of the study was the deposition of platinum on the obtained supports. For this, materials with close mass fractions of the metal component in the support were chosen. As was found earlier, the formaldehyde synthesis is the most suitable for the Pt/(SnO_2/C) catalysts preparation [21].

The Pt/(SnO_2/C) catalysts based on two supports SC-1 and SC_{CPL}-2 (hereinafter PSC-1 and PSC_{CPL}-2 respectively) were obtained by the formaldehyde method. They will be referred to as PSC-1 and PSC_{CPL}-2. Note that despite the same calculated mass fraction of platinum, its actual loading in the obtained materials turned out to be different (Table 2).

Comparison of X-ray patterns (Figure 3) and calculations using the Scherrer equation for PSC-1 and PSC_{CPL}-2 samples obtained under the same conditions show that the SnO_2 particle size in the PSC-1 sample is 1.5 times larger compared to the PSC_{CPL}-2 sample (Table 2).

This fact confirms the assumption that the addition of ε-caprolactam during the tin electrodeposition on a carbon support optimizes the particles' structure, reducing their size. Apparently, the ε-caprolactam additive also contributes to a more uniform surface distribution of platinum crystallites during the subsequent preparation of Pt/SnO_2/C catalysts.

SEM images of Pt/SnO_2/C samples (Figure 4 a) make it possible to trace some change in the surface morphology in the presence of CPL: the arrangement of

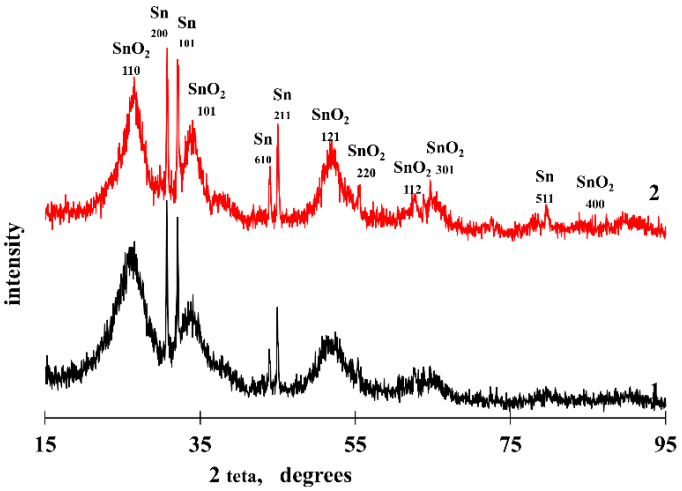

Figure 2 Typical X-ray diffraction patterns of SnO_2/C materials: 1 - SC_{CPL} -2, with the addition of ε-caprolactam during the deposition of tin on a dispersed carbon support; 2 - SC-1 without addition of ε-caprolactam.

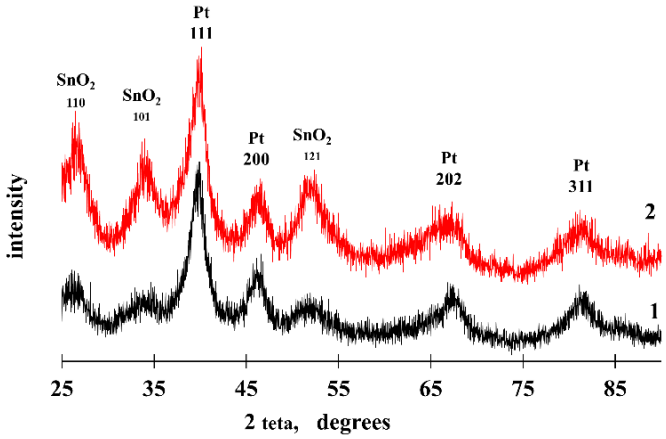

Figure 3 X-ray diffraction patterns of Pt/(SnO_2/C) materials: 1 - PSC_{CPL} - 2, 2 - PSC – 1.

tin oxide and platinum NPs is more uniform (Figure 4 b). The carbon support is agglomerates of rounded particles 50–100 nm in diameter. The Pt/(SnO_2/C) TEM image of the PSC_{CPL}-2 sample (Figure 4 c) demonstrates the uniformity of platinum and tin dioxide nanoparticles in the sample, and the histogram of the platinum nanoparticles size distribution (Figure 4 d) confirms the correctness of determining their sizes by X-ray diffraction (Table 2). A comparison of the structures of Pt/C and Pt/(SnO_2/C) catalysts, in which platinum was deposited by the same method, carried out in [30], showed that the aggregation of platinum nanoparticles is less. In the Pt/(SnO_2/C) catalyst PSC_{CPL}-2 the uniformity of the spatial distribution of platinum nanoparticles is also very high. Thus, the analysis of SEM and TEM microscopy data allows us to conclude that platinum is rather uniformly distributed and slightly agglomerated in the catalyst based on the SnO_2/C composite support obtained by tin electrode position with caprolactam additive (Figure 4).

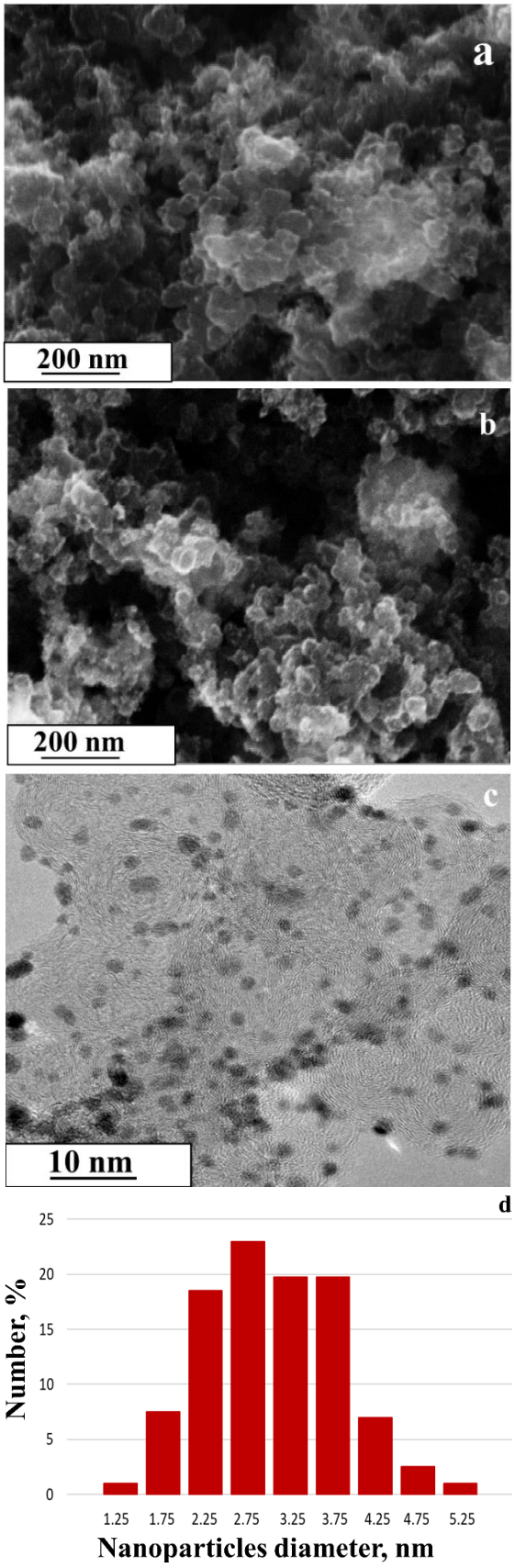

Figure 4 Photographs of the Pt/SnO_2/C samples surface obtained by scanning (scale – 200 nm) (a, b) and transmission (c) electron microscopy, and a histogram of the platinum nanoparticles size distribution (d) for a-PSC-l; b, c, d-PSC_{CPL}-2.

Cyclic voltammograms (CVs) of standardized electrodes used to calculate the ESA are shown in Figure 5. All CVs contain three regions, typically for platinum-containing catalysts. This is the region of hydrogen adsorption/desorption with peaks of strongly and weakly bound atoms (approximately 0–0.4 V); double-layer region corresponding to the charge/discharge of the EDL (approximately 0.3–0.6 V); area of platinum oxides formation/reduction (approximately 0.6–1.2 V) [31]. The large ESA value of the PSC_{CPL}-2 material (Table 3, Figure 5) associated with the prehistory of the PSC_{CPL}-2 material synthesis. It may be related to the use, the structure optimization of the electrolytic tin deposit under the ε-caprolactam influence, which may have a positive effect on the subsequent stages: the formation of tin oxide and more uniform distribution of platinum nanoparticles over the surface of the two-component support. It should be noted one more fact indirectly indicating a change in the carbon support properties after the deposition of SnO_2 on it from solutions containing caprolactam. Both the SnO_2/C composite support itself and the Pt/(SnO_2/C) catalyst based on it formed the most stable suspensions in water and isopropanol. Suspension stability may be due to the influence of "residual" caprolactam molecules absorbed on the carbon supports. It is possible that the porous layer formed from such a catalyst on the surface of the glass graphite disk electrode provides the best access of the reagent to the platinum nanoparticle.

When registering a series of potentiodynamic curves with a linear potential sweep (LSV) on a rotating disk electrode, the reaction rate of oxygen electroreduction, i.e. the mass activity of the catalyst was also maximum in

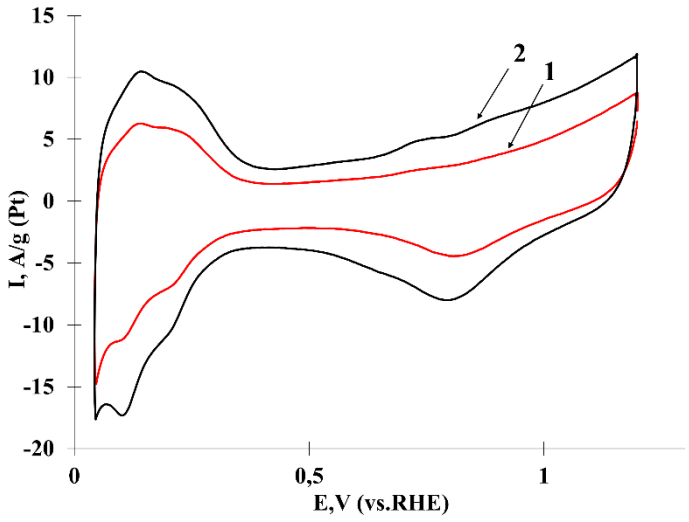

Figure 5 Cyclic voltammograms (2nd cycle) for 1 - PSC-l and 2 - PSC_{CPL} -2.

Table 3 – Some characteristics of the activity in ORR of PSC and PSCCPL catalyst.

Sample	ESA $H_{ads/des}$ $m^2/g(Pt)$	I_{mass}, $A \cdot g^{-1}$ (Pt) (E = 0.90 V)	I_{sp}, $A \cdot m^{-2}$ (Pt) (E = 0.90 V)	$E_{1/2}$	Number of *e* (E = 0.90 V)
PSC-1	40±3	233	7.3	0.91	3.5
PSC_{CPL}-2	56±7	291	5.2	0.92	4.3

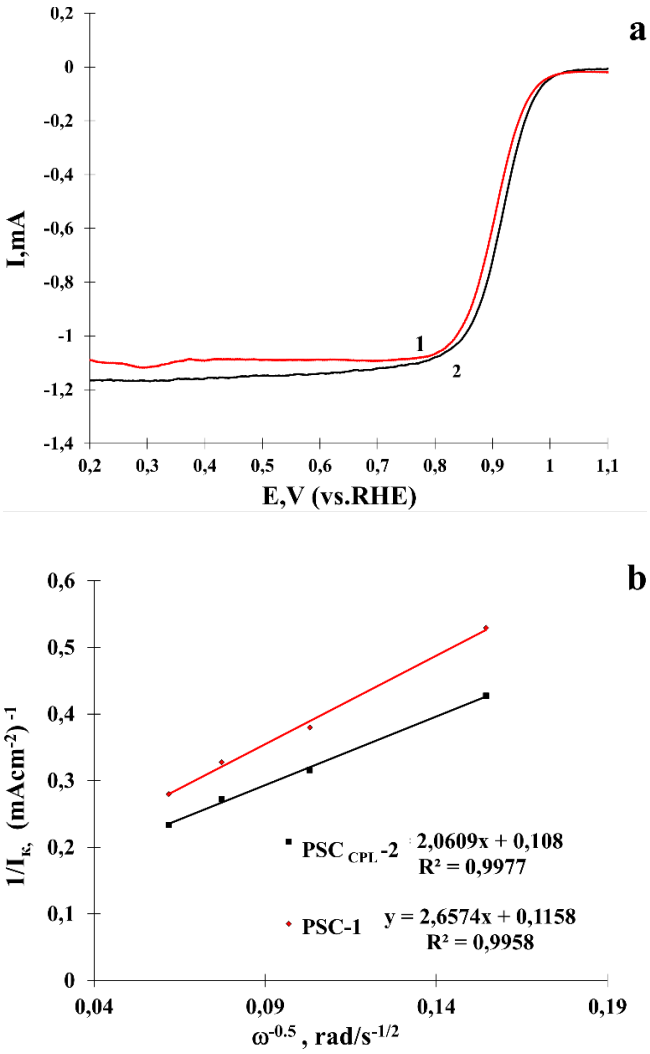

Figure 6 Linear sweep voltammograms of oxygen electroreduction in 0.1 M $HClO_4$ for 1-PSC-1 and 2 - PSC_{CPL} -2. Potential sweep rate - 20 mV/s, disk rotation - 1600 rpm. (b). Dependence of the reverse kinetic current at E = 0.9 V on ω-0.5 (b).

the case of the PSC_{CPL}-2 catalyst (Table 3, Figure 6). On this sample, the ORR begins at the most positive potentials (Figure 6, curve 2), which also manifests itself in a larger half-wave potential (Table 3).

As can be seen from Figure 6, the PSC_{CPL}-2 sample synthesized with the CPL addition at the tin electrodeposition stage has the highest activity among the studied objects. Extrapolation of ik-1, ω-0.5-straight to the *y*-axis for this catalyst gives the highest value of the kinetic current. The calculation of the number of electrons involved in the oxygen electroreduction reaction showed that for all the studied the value is close to ~ 4, which indicates a 4-electron mechanism of the process. Thus, the analysis of the obtained data on the activity of the obtained samples, summarized in Table 3, shows that the PSC_{CPL}-2 sample has the highest catalytic activity in ORR. Despite the same loading and size of platinum nanoparticles in the PSC-1 and PSC_{CPL}-2 samples, the latter is characterized by the highest ESA values and mass activity in ORR. We believe that the presence of CPL in the tin-plating electrolyte contributes not only to a decrease in the size of tin nanoparticles, which subsequently turn into oxide nanoparticles, but also to their more uniform distribution, which contributes to the subsequent uniform distribution of platinum crystallites (Figure 4).

4. Conclusions

In summary, composite SnO_2/C materials were obtained by tin electrodeposition on dispersed carbon particles. The presence of SnO_2 in the samples was confirmed by XRD and scanning electron microscopy. The addition of ε-caprolactam to the tin-plating electrolyte reduces the amount of tin deposited on dispersed carbon supports and reduces the size of SnO_2 crystallites formed during spontaneous oxidation of the tin crystallites. Platinum deposition on the composite SnO_2/C support surface makes it possible to obtain catalytically active Pt/(SnO_2/C) materials with a high ESA. In the case of using SnO_2/C support obtained in a CPL-containing electrolyte, the ESA and the mass activity of the Pt/(SnO_2/C) catalyst are the highest. This may be due to the optimization of the size and spatial distribution of nanoparticles at the stage of tin electrodeposition, which results in an increase in the uniformity of the distribution of subsequently formed platinum nanoparticles. Without excluding the possibility of partial dissolution of tin dioxide in the process of studying the electrochemical behavior of Pt/(SnO_2/C) materials. We note that we did not observe a decrease in the electrocatalysts activity in ORR. We can also conclude that the electrochemical behavior of Pt/(SnO_2/C) materials is similar to platinum-carbon catalysts.

Supplementary materials

No supplementary materials are available.

Funding

This research was financially supported by the Ministry of Science and Higher Education of the Russian Federation (State assignment in the field of scientific activity No 0852-2020-0019).

Acknowledgments

None.

Author contributions

Dmitry Mauer: Conceptualization; Data curation; Formal Analysis; Writing – review & editing.

Sergey Belenov: Investigation; Methodology; Supervision; Validation; Writing – original draft.

Conflict of interest

The authors declare no conflict of interest.

References

1. Thompsett D, Catalysts for the proton exchange membrane fuel cell, Eds: Vielstich, W., N.Y.: Wiley & Sons, **3** (2003) 6–23. https://doi.org/10.1201/9781420041552

2. Zhang J, Wang X, Wu C, Preparation and characterization of Pt/C catalysts for PEMFC cathode: effect of different reduction methods, React. Kinet. Catal. Lett. **83** (2004) 229–236. https://doi.org/10.1023/B:REAC.0000046081.96554.ae

3. Chen J, Jiang C, Yang X, Feng L, et al., Studies on how to obtain the best catalytic activity of Pt/C catalyst by three reduction routes for methanol electro-oxidation, Electrochem. Comm. **13** (2011) 314–316. https://doi.org/10.1016/j.elecom.2011.01.012

4. Prabhuram J, Zhao T, Wong C, Guo J, Synthesis and physical/electrochemical characterization of Pt/C nano-catalyst for polymer electrolyte fuel cells, J. Pow. Sources **134** (2004) 1–6. https://doi.org/10.1016/j.jpowsour.2004.02.021

5. Guterman VE, Novomlinskij IN, Skibina LM, Mauer DK, Method for Obtaining Nanostructural Material of tin Oxide on Basis of Carbon. Russian Federation patent RUS 2656914. 2018 June 7.

6. Novomlinskij IN, Volochaev VA, Tsvetkova GG, Guterman VE, New electrochemical method for the preparation of Pt/C nanostructured materials, Cond. Matter Interphas. **19** (2017) 112-119. https://doi.org/10.17308/kcmf.2017.19/11

7. Kuriganova AB, Leontyeva DV, Ivanov S, et al., Electrochemical dispersion technique for preparation of hybrid MOx–C supports and Pt/MOx–C electrocatalysts for low-temperature fuel cells, J. Appl. Electrochem. **46** (2016) 1245–1260. https://doi.org/10.1007/s10800-016-1006-5

8. Zhang K, Feng C, He B, Dong H, Dai W, et al., An advanced electrocatalyst of Pt decorated SnO_2/C nanofibers for oxygen reduction reaction, J. Electroanalyt. Chem. **781** (2016) 198–203. https://doi.org/10.1016/j.jelechem.2016.11.002

9. Dahl PI, Barnett AO, Monterrubio FA, Colmenares LC, The use of tin oxide in fuel cells, In: Tin oxide materials, Elsevier. **781** (2020) 379–410. https://doi.org/10.1016/B978-0-12-815924-8.00013-X

10. Santos AO, Silva JCM, Antoniassi RM, Ponzio EA, et al., The format electrooxidation on Pt/C and PtSnO_2/C nanoparticles in alkaline media: The effect of morphology and SnO_2 on the platinum catalytic activity, Int. J. Hydr. Ener. **45** (2020) 33895–33905. https://doi.org/10.1016/j.ijhydene.2020.08.165

11. Mensharapov RM, Ivanova N A, Spasov D D, Kukueva EV, et al., Carbon-supported Pt-SnO_2 catalysts for oxygen reduction reaction over a wide temperature range: Rotating disk electrode study, Catalysts. **11** (2021) 1469. https://doi.org/10.3390/catal11121469

12. Hussain S, Kongi N, Erikson H, Rähn M, et al., Platinum nanoparticles photo-deposited on SnO_2-C composites: An active and durable electrocatalyst for the oxygen reduction reaction, Electrochim. Acta. **316** (2019) 162–172. https://doi.org/10.1016/j.electacta.2019.05.104

13. Chao G, An X, Zhang L, Tian J, et al., Electron-rich platinum electrocatalysts supported onto tin oxides for efficient oxygen reduction, Composites Commun. **24** (2021) 100603. https://doi.org/10.1016/j.coco.2020.100603

14. Shen X, Nagai T, Yang F, Zhou L, et al., Dual-site cascade oxygen reduction mechanism on SnO_x/Pt–Cu–Ni for promoting reaction kinetics, J. Am. Chem. Soc. **141** (2019) 9463–9467. https://doi.org/10.1021/jacs.9b02286

15. Madhu SS, Ruying L, Mei C, Xueliang S, High electrocatalytic activity of platinum nanoparticles on SnO_2 nanowire-based electrodes, Electrochem. Solid-State Lett. **10** (2007) B130-B133. https://doi.org/10.1149/1.2745632

16. Lee JH, Park SJJ, Preparation of spherical TiO_2/SnO_2 powders by ultrasonic spray pyrolysis and its spinodal decomposition, Am. Ceram. Soc. **76** (1993) 254–258. https://doi.org/10.1007/BF00179220

17. Williams G, Coles GSV, Gas sensing properties of nanocrystalline metal oxide powders produced by a laser evaporation technique, J. Mater. Chem. **8** (1998) 1657–1664. https://cronfa.swan.ac.uk/Record/cronfa26914

18. Willett MJ, Burganos VN, Tsakiroglou CD, Payatakes AC, Nanocrystalline oxides for gas, sensing, Sens. Actuators. (1998) B 53–76. https://doi.org/10.1007/0-306-47609-6_7

19. Zhang J, Gao L, Synthesis of SnO_2 Nanoparticles by the sol-gel method from granulated tin, Chem. Lett. **32** (2003) 458–459. https://doi.org/10.1246/cl.2003.458

20. De Monredon S, Cellot A, Ribot F, Sanchez C, et al., Synthesis and characterization of crystalline tin oxidenanoparticles, J. Mater. Chem. **12** (2002) 2396–2400. https://doi.org/10.1039/B203049G

21. Song KC, Kang Y, Preparation of high surface area tin oxide powders by a homogeneous precipitation method, Mater. Lett. **42** (2000) 283–289. https://doi.org/10.1016/S0167-577X(99)00199-8

22. Meiling D, Ming H, Dong Li, Wangting L, et al., SnO_2 nanocluster supported Pt catalyst with high stability for proton exchangemembrane fuel cells, Electrochim. Acta. **92** (2013) 468–473. https://doi.org/10.1016/j.electacta.2013.01.070

23. Skibina LM, Mauer DK, Sokolenko, The effect of cyclic lactams and their structural analogs on the surface morphology, coating properties, and electroreduction kinetics of Cu(II) ions, Protec. Metals Phys. Chem. Surf. **54** (2018) 624–631. https://doi.org/10.1134/S2070205118030164

24. Skibina LM, Kuznetsov VV, Sukholentsev EA, The effect of the ε-caprolactam concentration on the electrodeposition of nickel–polymer coatings, Protec. Metals. **37** (2001) 159–162. https://doi.org/10.1023/A:1010330222922

25. Novomlinski IN, Tabachkova NY, Safronenko OI, Guterman VE, Novel electrochemical method for the preparation of Pt/C nanostructured material, Monatshefte Für Chemie - Chemical Monthly. **150** (2019) 631–637. https://doi.org/10.1007/s00706-019-2383-3

26 Shinozaki K, Zack JW, Pylypenko S, Pivovar BS, et al., Oxygen reduction reaction measurements on platinum electrocatalysts utilizing rotating disk electrode technique, J. Electrochem. Soc. **162** (2015) 1384–1396. https://doi.org/10.1149/2.1071509jes

27. Suryanarayana C, Norton MG, X-ray diffraction: a practical approach, Springer Science & Business Media. (2013) 273. https://doi.org/10.1007/978-1-4899-0148-4

28. Gražulis S, Daškevič A, Merkys A, Chateigner, et al., Crystallography Open Database (COD): an open-access collection of crystal structures and platform for world-wide collaboration Nucleic Acids Research, **40** (2012) D420–D427. https://doi.org/10.1093/nar/gkr900

29. Klug HP, Alexander LE, X-Ray Diffraction procedures: for polycrystalline and amorphous materials, 2nd Edition John Wiley: New York USA, (1974) 992.

30. Novomlinskiy IN, Danilenko MV, Safronenko OI, Tabachkova NY, et al., Influence of the Sn-oxide-carbon carrier composition on the functional characteristics of deposited platinum electrocatalysts, Electrocatalys. **12** (2021) 489–498. https://doi.org/10.1007/s12678-021-00649-8

31. Savinova DV, Molodkina EB, Danilov AI, Polukarov YM, Surface and subsurface oxygen on platinum in a perchloric acid solution, Rus. J. Electrochem. **40** (2004) 683–687. https://doi.org/10.1023/B:RUEL.0000035248.39620.f